EXPERIMENTAL STUDY ON THE SHEAR BEHAVIOR OF FRCM STRENGTHENED MASONRY PANELS

FRANCESCA FERRETTI[1*], ANDREA INCERTI[2] AND CLAUDIO MAZZOTTI[1]

[1] Department of Civil, Chemical, Environmental and Materials Engineering (DICAM)
University of Bologna
Viale Risorgimento 2, 40136 Bologna, Italy
e-mail: francesca.ferretti10@unibo.it (*corresponding author), claudio.mazzotti@unibo.it

[2] CIRI Buildings and Construction (CIRI-EC)
University of Bologna
Via del Lazzaretto 15/5, 40131 Bologna, Italy
e-mail: a.incerti@unibo.it

Keywords: Masonry, In-plane Shear Behavior, Brick, FRCM, Strengthening

Abstract. *Innovative strengthening solutions, such as Fiber Reinforced Cementitious Matrix (FRCM), are becoming increasingly diffused for the retrofitting of existing masonry structures with the aim of reducing the seismic vulnerability of these construction typologies. In recent years, many studies have demonstrated the suitability of these materials in enhancing the shear capacity of masonry walls and improve the overall structural behavior, avoiding fragile collapse mechanisms. In the present work, six diagonal compression tests were performed on unstrengthened and FRCM strengthened masonry panels to evaluate the improvements attributable to the presence of the FRCM systems. Two different bidirectional basalt grids were applied to the masonry samples, with and without mechanical anchorages. The tensile and bond properties of the chosen FRCM systems were investigated through laboratory tests. The objective was, indeed, to compare the performances of two textiles, characterized by different densities, and to investigate the role of mechanical anchorages. The experimental results confirmed the efficiency of the FRCM strengthening systems in improving the shear behavior of masonry panels. The FRCM strengthened samples experienced a considerable strength increase and less brittle failure mechanisms. The roles of both the mortar matrix, the fiber grids and the mechanical anchorages were highlighted by analyzing the onset of cracking and the failure propagation within the samples.*

1 INTRODUCTION

The structural performances and the safety of historical masonry building during a seismic event are key aspects to be assessed, since these construction typologies usually show a weak behavior if subject to horizontal loads, characterized by out-of-plane and in-plane collapses [1,2]. Several researches in literature studied different retrofitting systems realized by using composite materials applied to the surface of masonry elements, in order to enhance the structural capacity with respect to the shear actions invoked during an earthquake without

evident changes in stiffness.

In this framework, Fiber Reinforced Polymer (FRP) or Fiber Reinforced Cementitious Matrix (FRCM) systems were introduced and their advantages and drawbacks highlighted [3-5]. The behavior of these innovative materials was broadly analyzed with reference to the resistance, i.e. tensile and bond strength, the influence of the masonry substrate, e.g. presence of mortar joint and brick roughness, their compatibility with the substrate, the sustainability, and the fire resistance [6-13]. Studies were also carried out about the in-plane behavior of masonry walls, made of different masonry substrates, strengthened with composite materials [14-21]. From the structural point of view, the efficiency of these systems was found to be highly significant.

The aim of the present research is to enhance the knowledge about the structural performances and the failure modes of masonry panels, built with clay bricks and lime-based mortar, strengthened with FRCM systems made with bidirectional basalt fiber grids and a lime-based mortar matrix. To this aim, a diagonal compression test setup [22,23] was adopted to analyze the in-plane shear behavior of the wall panels. The experimental results obtained were discussed in terms of load bearing capacity and maximum displacement at collapse, considering the effectiveness of the FRCM strengthening systems with respect to the unreinforced masonry samples.

2 EXPERIMENTAL CAMPAIGN

In the present experimental campaign, two different masonry substrates were investigated, built with the same fired clay bricks and two different mortar mixes (*B-M1* and *B-M2*). The masonry panel dimensions were equal to $1100 \times 1100 \times 250$ mm^3 and $1200 \times 1200 \times 250$ mm^3 for the *B-M1* and *B-M2* typology, respectively. Six masonry walls were built, three for each substrate type. Subsequently, four panel were retrofitted by FRCM composites, made with a lime-based mortar matrix and bidirectional basalt fiber grids. The characteristics of the tested samples are reported in Table 1, where each specimen is named with a code indicating the wall substrate type (*B-M1* or *B-M2*), the applied FRCM system (basalt fiber grids, *B200* or *B400*, and mortar matrix type, *M3* or *M4*) and the presence of mechanical anchorages (*A*) or not. A continuous layout of the strengthening system was adopted (Figure 1): the bidirectional basalt grids were applied symmetrically on the entire surfaces of the wall panels, adopting an offset of about 20 mm from edges to prevent early debonding phenomena. A single grid layer per side was adopted, embedded in a 6 mm thick layer of mortar. A total number of six diagonal compression tests were performed. The mechanical characterization of the masonry components and the FRCM strengthening systems will be presented in the following Sections.

Table 1: Experimental campaign: characteristics of the tested samples

Specimen ID	FRCM system	Mechanical Anchorages
B-M1_URM	-	-
B-M2_URM	-	-
B-M1_B200-M3-A		Yes
B-M2_B200-M4	Basalt fiber grid +	-
B-M1_B400-M3-A	NHL mortar matrix	Yes
B-M2_B400-M4		-

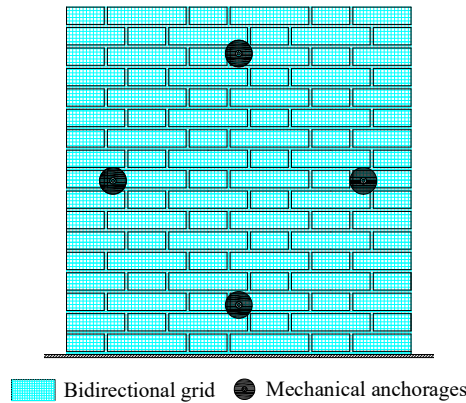Bidirectional grid   ● Mechanical anchorages

Figure 1: FRCM strengthening system layout

2.1 Masonry constituents

The fired clay bricks adopted for the construction of the masonry panels had dimensions equal to $120 \times 250 \times 55$ mm^3. Their mechanical properties were investigated through standard laboratory tests. In particular, uniaxial compressive tests [24] and Brazilian tests [25] were carried out on cylindrical specimens with a unitary aspect ratio, obtaining a compressive strength $f_{c,b}$ equal to 18.7 MPa (CoV = 5%) and a tensile strength $f_{t,b}$ equal to 3.1 MPa (CoV = 15%). Moreover, three-points bending tests [26] were performed on prismatic specimens, having dimensions $40 \times 40 \times 250$ mm^3, for the evaluation of the flexural strength $f_{fl,b}$, obtaining 4.8 MPa (CoV = 7%). Finally, also the elastic modulus was determined through cyclic compression tests [27], resulting to be equal to 6850 MPa (CoV = 3.9%).

Concerning the mortar used in the masonry bed joints, two mortar typologies were adopted for the construction of the brick masonry panels (*M1* and *M2*). They were pre-mixed natural hydraulic lime-based mortars and they were subject to standard laboratory tests for the mechanical characterization [28], obtaining the mechanical properties reported in Table 2 in terms of compressive strength ($f_{c,m}$), flexural strength ($f_{fl,m}$) and elastic modulus (E_m).

Table 2: Mechanical properties of the mortars

Mortar	$f_{c,m}$ (MPa)	CoV (%)	$f_{fl,m}$ (MPa)	CoV (%)	E_m (MPa)	CoV (%)
M1	4.8	12	1.5	15	4590	17
M2	2.6	12	1.2	9	4250	18

2.2 Strengthening systems and layout

Two different FRCM retrofitting systems were investigated, constituted of bidirectional symmetrical basalt fiber grids embedded in a natural hydraulic lime-based mortar matrix. The grids were characterized by different density, equal to 200 g/m^2 (*B200*) and 400 g/m^2 (*B400*), and equivalent thicknesses equal to 0.032 mm and 0.064 mm, respectively. Pre-mixed natural hydraulic lime-based mortars were adopted as matrix (*M3* and *M4*), characterized by the mechanical properties reported in Table 3, evaluated through standard tests [28].

At the beginning of the experimental campaign, the adopted FRCM strengthening systems

were subject to direct tensile tests in order to evaluate the tensile strength $f_{t,f}$, the ultimate strain ε_u and the fiber elastic modulus E_f. Moreover, direct shear tests [6] were also performed to determine the bond strength $f_{b,f}$. The experimental outcomes of tensile and bond tests are reported in Table 4 and Table 5, respectively.

The efficiency η of the basalt FRCM systems was evaluated as the ratio between the bond strength and the tensile strength (Table 5): the highest value (91%) was associated to the textile failure due to fiber rupture (*B200*), while the lowest value (64%) was observed for the textile showing a delamination at the matrix-fiber interface (*B400*).

Table 3: Mechanical properties of the mortar matrices

Mortar	$f_{c,m}$ (MPa)	CoV (%)	$f_{fl,m}$ (MPa)	CoV (%)	E_m (MPa)	CoV (%)
M3	12.6	9	2.9	23	9100	14
M4	13.1	5	3.4	5	8675	11

Table 4: FRCM systems: results of the tensile tests

Textile	Fiber type	Specimen dimensions (mm³)	$f_{t,f}$ (MPa)	ε_u (%)	E_f (GPa)
B200	Basalt grid	400×40×10	1160	2.2	76
B400	Basalt grid	400×40×10	960	1.1	66

Table 5: FRCM systems: results of the direct shear tests

Textile	Masonry prism (mm³)	Bonded length (mm)	Bonded width (mm)	Thickness (mm)	$f_{b,f}$ (MPa)	η (%)
B200	120×120×445	345	50	8	1060	91
B400	120×120×445	345	50	8	620	64

3 DIAGONAL COMPRESSION (DC) TEST SETUP

The experimental setup used to evaluate the shear capacity of the clay brick masonry walls was a standard setup, following the indications provided by the ASTM E519 and RILEM LUMB6 Standards [22,23]. A servo-hydraulic actuator, equipped with a load cell having a maximum capacity of 500 kN, was used for the application of the diagonal compression displacement. The tests were, indeed, performed under displacement control with a rate equal to 0.01 mm/s to analyze both the pre-peak and the post-peak behavior. The diagonal displacements were measured by four linear potentiometers (50 mm stroke and 1100 mm gage length), positioned on both sides of the masonry panels along the two principal diagonals. The setup of the test is shown in Figure 2. In accordance with the elastic solution of a masonry panel subject to a DC test [29,30], the stress state (σ, τ) in the center of the panel and the masonry tensile strength f_t can be evaluated as:

$$\sigma = 0.56 \frac{P}{A_n} \tag{1}$$

$$\tau = 1.05 \frac{P}{A_n} \tag{2}$$

$$f_t = 0.5 \frac{P_f}{A_n} \tag{3}$$

where P is the diagonal load (P_f at failure) and A_n is the net area of the wall. In this configuration, the directions of the principal stresses are known and coincident with the diagonals of the panels. The shear strain γ can be determined as the sum of the deformations evaluated along the principal directions (ε_c and ε_t), taken as the average between the deformations on the two sides of the specimen. Considering the tangential stress τ *vs* shear strain γ diagram, the shear modulus G can be evaluated as the secant modulus between 1/10 and 1/3 of the maximum tangential stress.
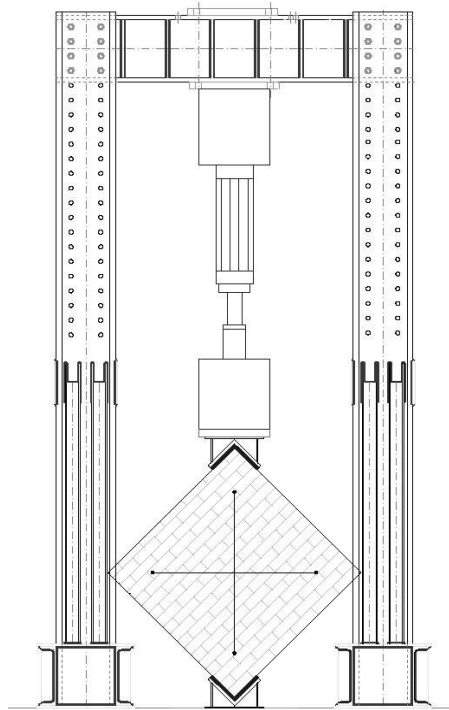

Figure 2: Diagonal compression (DC) test setup.

4 EXPERIMENTAL RESULTS

The experimental results are presented and discussed in this Section in terms of shear behavior, shear capacity and failure mode with the objective of discussing the improvements given by the FRCM composites applied on unreinforced masonry.

4.1 Failure modes

During the DC tests, two different failure modes occurred, reported in Figure 5. In particular, the failure modes of the URM panels were characterized by an evident single fracture line along the compressed diagonal, according to the panel stress state (Figure 5a). The FRCM strengthened masonry walls, instead, showed a more widespread cracking pattern on the external surfaces of the reinforcing layers, along the compressed diagonal. With reference to the failure mode of the FRCM reinforcements, it was noticeable that the *B200* basalt grid (Figure 5b,d) was characterized by partial delamination and rupture of fibers along the cracking lines (Figure 5f), while the failure of the *B400* basalt grid was characterized by delamination phenomena only. This different behavior can be related to the reduced spacing of the *B400* grid, which did not allow the mortar matrix to properly penetrate within the grid itself. The presence of the mechanical anchorages did not significantly influence the overall behavior of the samples in terms of failure mode, but it prevented the grid detachment at the extremities of the wall panels, which was visible for the samples strengthened without the use of anchorages.
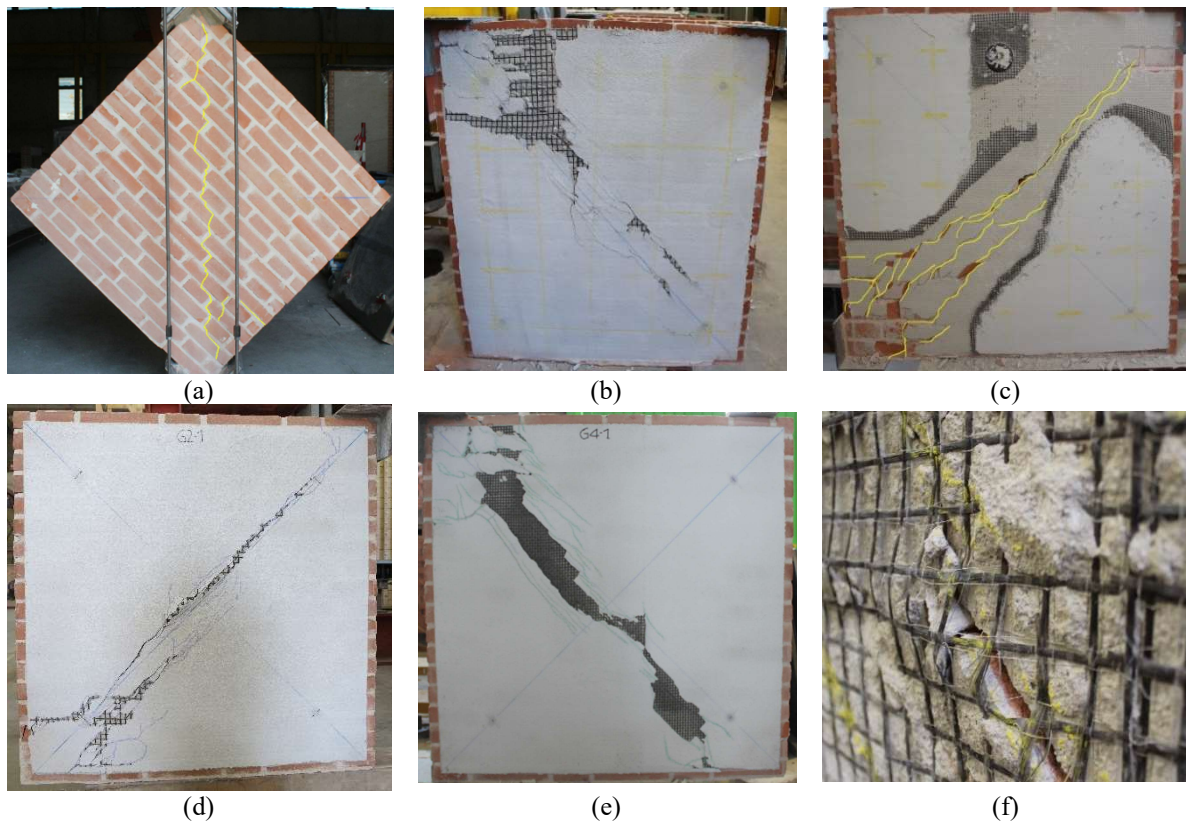

(a) (b) (c)

(d) (e) (f)

Figure 5: Failure modes in the DC tests: (a) URM panel; (b) B-M1_B200-M3-A; (c) B-M1_B400-M3-A; (d) B-M2_B200-M4; (e) B-M2_B400-M4; (f) delamination and rupture of the *B200* textile.

6

4.2 Shear behavior and capacity of the FRCM strengthened panels

The load *vs* displacements graphs are reported in Figure 3 and Figure 4 for the *B-M1* and *B-M2* panel series, respectively. A very similar shear behavior was noticed, characterized by an initial linear branch and a first peak load, followed by a drop in the load bearing capacity and by a second peak load. From the experimental observations, it can be stated that the reaching of the first peak load corresponded with the appearance of the first crack in the mortar matrix. The second peak load, instead, can be associated with the failure of the textiles.

The results of the DC tests are summarized in Table 6, in terms of diagonal load at failure P_f, strength increment with respect to URM panel, masonry tensile strength f_t, shear modulus G and pseudo-ductility μ. The latter was determined as the ratio between the ultimate shear strain, taken in correspondence of a 20% reduction in the load bearing capacity after the peak load, and the shear strain corresponding to the same load value along the initial loading branch.
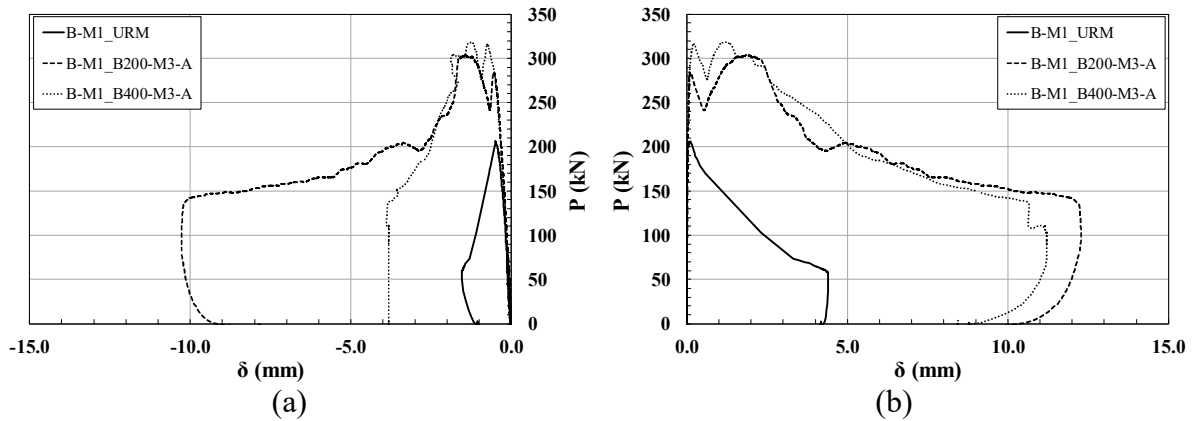

Figure 3: DC test results for *B-M1* panels: (a) Load *vs* vertical displacement graph; (b) Load *vs* horizontal displacement graph
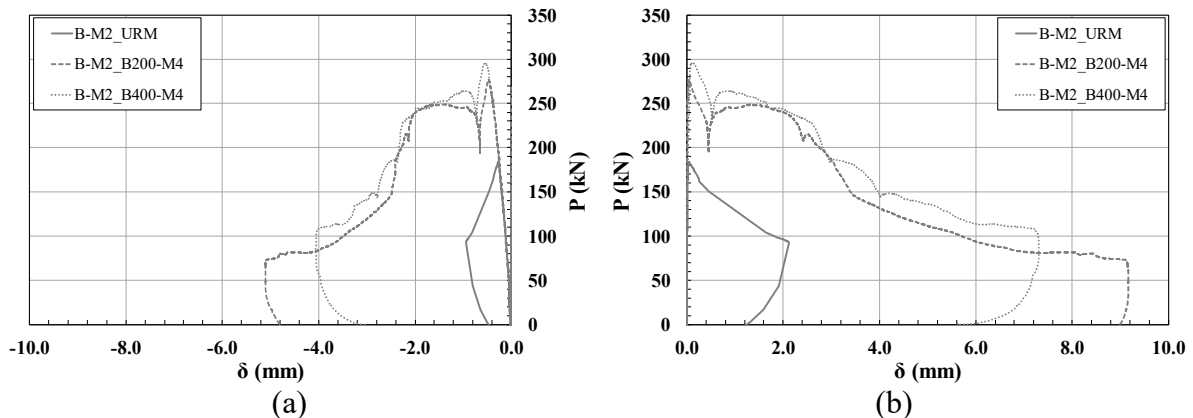

Figure 4: DC test results for *B-M2* panels: (a) Load *vs* vertical displacement graph; (b) Load *vs* horizontal displacement graph

7

Table 6: Diagonal compression test results.

Sample code	P_f (kN)	Strength Increment (%)	τ_f (MPa)	$f_{t,M}$ (MPa)	$G_{1/10-1/3}$ (MPa)	μ (-)
B-M1_URM	206.1	-	0.79	0.37	2660	4.0
B-M2_URM	183.7	-	0.64	0.30	3056	4.4
B-M1_B200-M3-A	303.7	47	1.16	0.55	2649	13.9
B-M2_B200-M4	276.7	51	0.96	0.46	3216	13.3
B-M1_B400-M3-A	318.7	55	1.22	0.58	2810	10.9
B-M2_B400-M4	295.8	61	1.04	0.49	2705	10.9

With regards to the results obtained for the two URM panels, the differences observed in the maximum load and, consequently, in the masonry tensile strength, can be associated to the differences in the mechanical properties of the mortar used for the construction of the panels, e.g. $f_{c,m(B-M1)} > f_{c,m(B-M2)}$.

With reference to the results obtained for FRCM strengthened samples, it is possible to state that, for both the masonry typologies, significant strength increments were obtained. In particular, similar increments were observed for panels strengthened with the same FRCM system, given that the mortar matrices *M3* and *M4* were characterized by similar mechanical properties. It is worth mentioning that the strength increments obtained for the panels strengthened with the *B400* basalt grid were not as high as expected, given that the *B400* grid was characterized by an amount of fibers doubled with respect to the *B200* grid. It should be considered that the efficiency of the *B400* textile was significantly lower, as reported in Table 5: the bond strength was approximately equal to half the tensile strength of the *B200* grid. This observation could explain why a similar strength increment was registered in the DC tests for the panels strengthened with the two FRCM typologies.

The presence of the mechanical anchorages seems not to significantly affect the value of the first peak load. However, they influenced the behaviour after the first peak. Indeed, the mechanical anchorages, and generally the fiber grids, started working in the second reloading branch. More in detail, the panels strengthened making use of anchorages experienced a higher load increment after the first peak, reaching a second peak load similar or even higher than the first one.

Values of the shear modulus *G* for the masonry panels were quite similar, demonstrating that the structural performances were enhanced by the application of the FRCM retrofitting systems without considerable changes in terms of stiffness, with values ranging between 2649 and 3216 MPa.

Finally, the displacement capacity of the FRCM strengthened samples was significantly higher than the one of the URM samples, which experienced a quasi-brittle failure. Quite high values of the pseudo-ductility factor μ were, indeed, evaluated for all the FRCM strengthened panels. In particular, similar results were obtained for walls strengthened with the same FRCM system. The pseudo-ductility was higher for the panels strengthened by the *B200* textile, most probably for the same reasons introduced above: failure mode and efficiency of the grid.

5 ANALYTICAL FORMULATION

The evaluation of the shear capacity of strengthened walls ($\tau_{t,r}$) can be carried out through the anaytical formulation provided by the Italian CNR Guideline for the design of strengthening interventions using FRCM systems [31]. The formulation is based on an additive approach, considering the contributions of unreinforced masonry ($\tau_{f,URM}$) and of the dry fibers ($\tau_{t,f}$), according to Equation (4):

$$\tau_{t,r} = \tau_{f,URM} + \tau_{t,f} = \tau_{f,URM} + \frac{n_f \cdot t_{Vf} \cdot l_f \cdot \alpha_t \cdot E_f \cdot \varepsilon_{fd}}{\gamma_{Rd} \cdot A_n} \qquad (4)$$

where τ_f is here considered equal to the shear strength of the correspondent URM sample, n_f is the number of reinforcing layers, t_{vf} is the textile equivalent thickness, l_f is the width of the FRCM system measured orthogonally to the shear force, α_t is a coefficient, equal to 0.8, accounting for a reduced tensile strength for fibers subjected to shear, E_f is the fiber elastic modulus, ε_{fd} is the design strain of the FRCM system, γ_{Rd} is a safety factor, considered equal to 1 here, and A_n is the net area of the panel cross section. In detail, the design strain is considered equal to the ratio between the bond strength and the elastic modulus E_f of the dry fibers, for the panels strengthened without using mechanical anchorages, while it is multiplied by 1.5 for the panels reinforced with mechanical anchorages, to account for intermediate delamination phenomena.

The analytical and experimental results are compared in Table 7, where the maximum shear stress obtained in the DC test ($\tau_{f,Exp}$) is reported together with the shear capacity of the strengthened walls, calculated according to Equation (4). The analytical formulation generally underestimates the experimental outcomes, even if a quite good agreeement can be noticed between experimental and analytical results. However, it should be mentioned that the proposed analytical formulation does not take into account the role of the mortar matrix, which was found to be crucial in the experimental tests. Indeed, especially for the panel series *B-M2*, the maximum shear stress was reached in correspondence of the first peak load, related to the cracking of the mortar matrix and not to the failure of the textile.

Table 7: Shear capacity of FRCM strengthened panels: analytical *vs* experimental results.

Sample code	$\tau_{f,URM}$ (MPa)	$\tau_{t,f}$ (MPa)	$\tau_{t,r}$ (MPa)	$\tau_{f,Exp.}$ (MPa)	Error (%)
B-M1_B200-M3-A	0.79	0.31	1.10	1.16	-5.2
B-M2_B200-M4	0.64	0.21	0.85	0.96	-11.5
B-M1_B400-M3-A	0.79	0.29	1.07	1.22	-12.3
B-M2_B400-M4	0.64	0.25	0.89	1.04	-14.4

6 CONCLUSIONS

The present research deals with the study of the shear behavior of FRCM strengthened

masonry panels through the execution of DC tests. Six masonry panels were built, and two masonry typologies were considered. Four panels were then strengthened adopting two different FRCM systems, both characterized by the use of basalt bidirectional grids, having different densities, and a lime-based mortar matrix. The effect of the presence of mechanical anchorages on the shear strength of the masonry samples was also analyzed.

The experimental results showed a good efficiency of the strengthening systems, with strength increments ranging from 47% to 61%, with respect to the URM panels. The presence of the FRCM systems did not determine significant stiffness increase of the panels but it influenced their failure mode, which became more ductile if compared to the quasi-brittle failure of the URM samples. The pseudo-ductility factor was indeed evaluated in the experimental campaign.

In general, the shear behavior of the FRCM strengthened samples was characterized by a first peak load, corresponding to the cracking of the mortar matrix, and by a second peak load, associated to the failure of the textiles. The role of the mortar matrix was highlighted since it was found to be crucial in the shear behavior of the strengthened panels. The presence of the mechanical anchorages seemed not to significantly affect the failure mode of the panels and the value of the first peak load. However, the anchorages allowed the textile to better redistribute the tensile stresses and determined a higher load increment after the drop in the load bearing capacity following the first peak load.

A comparison between the experimental results and the analytical formulation provided by the Italian CNR Guideline was carried out, showing a quite good agreement. In particular, the analytical results tended to underestimate the experimental ones. In general, it should be mentioned that the important role of the mortar matrix is not taken into account by the available analytical formulation. Further experimental results are needed to better analyze the matrix contribution and maybe include it in an alternative analytical approach.

REFERENCES

[1] Penna, A., Morandi, P., Rota, M., Manzini, C.F., da Porto, F. and Magenes G. Performance of masonry buildings during the Emilia 2012 earthquake. Bull. Earthq. Eng. (2014) 12:2255–73. https://doi.org/10.1007/s10518-013-9496-6.

[2] Ferretti, F., Ferracuti, B., Mazzotti, C. and Savoia M. Destructive and minor destructive tests on masonry buildings: Experimental results and comparison between shear failure criteria. *Constr. Build. Mater.* (2019) **199**:12–29. https://doi.org/10.1016/j.conbuildmat.2018.11.246.

[3] Papanicolaou, C., Triantafillou, T., Karlos, K. and Papathanasiou M. Textile-reinforced mortar (TRM) versus FRP as strengthening material of URM walls: in-plane cyclic loading. *Mater. Struct.* (2007) **40**:1081–97. https://doi.org/10.1617/s11527-006-9207-8.

[4]   Papanicolaou, C., Triantafillou, T. and Lekka, M. Externally bonded grid as strengthening and seismic retrofitting materials of masonry panels. *Constr. Build. Mater.* (2011) **25**(2):504-514.

[5]   Mazzotti, C. and Murgo, F.S. Numerical and experimental study of GFRP-masonry interface behavior: Bond evolution and role of the mortar layers. *Compos. Part B Eng.* (2015) **75**:212–225.

[6]   De Felice, G., Aiello, M.A., Caggegi, C., Ceroni, F., De Santis, S., Garbin, E., et al. Recommendation of RILEM Technical Committee 250-CSM: Test method for Textile Reinforced Mortar to substrate bond characterization. *Mater. Struct.* (2018) **51**:95. https://doi.org/10.1617/s11527-018-1216-x.

[7]   Valluzzi, M.R., Oliveira, D.V., Caratelli, A., Castori, G., Corradi, M., de Felice, G., et al. Round Robin Test for composite-to-brick shear bond characterization. *Mater. Struct.* (2012) **45**:1761–91. https://doi.org/10.1617/s11527-012-9883-5.

[8]   Ceroni, F., de Felice, G., Grande, E., Malena, M., Mazzotti, C., Murgo, F., et al. Analytical and numerical modeling of composite-to-brick bond. *Mater. Struct.* (2014) **47**:1987–2003. https://doi.org/10.1617/s11527-014-0382-8.

[9]   de Felice, G., Aiello, M.A., Bellini, A., Ceroni, F., De Santis, S., Garbin, E., et al. Experimental characterization of composite-to-brick masonry shear bond. *Mater. Struct.* (2016) **49**:2581–96. https://doi.org/10.1617/s11527-015-0669-4.

[10]   Carozzi, F.G., Bellini, A., D'Antino, T., de Felice, G., Focacci, F., Hojdys, Ł., et al. Experimental investigation of tensile and bond properties of Carbon-FRCM composites for strengthening masonry elements. *Compos. Part B Eng.* (2017) **128**:100–19. https://doi.org/10.1016/j.compositesb.2017.06.018.

[11]   Sassoni, E., Andreotti, S., Bellini, A., Mazzanti, B., Bignozzi M.C., Mazzotti, C. and Franzoni E. Influence of mechanical properties, anisotropy, surface roughness and porosity of brick on FRP debonding force. *Compos. Part B* (2017) **108**:257-269.

[12]   Lignola, G.P., Caggegi, C., Ceroni, F., De Santis, S., Krajewski, P., Lourenço, P.B., Morganti, M., Papanicolaou, C., Pellegrino, C., Prota, A., and Zuccarino, L. Performance assessment of Basalt FRCM for retrofit applications on masonry. *Compos. Part B* (2017) **128**:1-18.

[13]   Bellini, A., Bovo, M. and Mazzotti, C. Experimental and numerical evaluation of fiber-matrix interface behaviour of different FRCM systems. *Compos. Part B* (2019) **161**:411-426.

[14]   Faella, C., Martinelli, E., Nigro, E. and Paciello, S. Shear capacity of masonry walls externally strengthened by a cement-based composite material: an experimental campaign. *Constr. Build. Mater.* (2010) **25**:4403–4414.

[15]   Babaeidarabad, S., De Caso, F. and Nanni, A. URM Walls Strengthened with Fabric-Reinforced Cementitious Matrix Composite Subjected to Diagonal Compression. *J. Compos. Constr.* (2014) **18**:04013045. https://doi.org/10.1061/(ASCE)CC.1943-5614.0000441.

[16]   Ferretti, F., Incerti, A., Ferracuti, B. and Mazzotti, C. FRCM strengthened masonry panels: the role of mechanical anchorages and symmetric layouts. *Key Eng. Mater.* (2017) **747**:334–341.

[17]   Incerti, A. Tilocca, A.R., Ferretti, F. and Mazzotti, C. Influence of masonry texture on the shear strength of FRCM reinforced panels. In: R. Aguilar et al. (Eds.): *Structural Analysis of Historical Constructions*, RILEM Bookseries 18 (2019), pp. 1623-1631.

[18]   Ferretti, F., Incerti, A., Tilocca, A.R. and Mazzotti, C. In-Plane Shear Behavior of Stone Masonry Panels Strengthened through Grout Injection and Fiber Reinforced Cementitious Matrices. *Int. J. Archit Herit.* (2019). https://doi.org/10.1080/15583058.2019.1675803.

[19]   Incerti A., Ferretti F. and Mazzotti C. FRCM strengthening systems efficiency on the shear behavior of pre-damaged masonry panels: an experimental study. *J. Build. Pathol. Rehabil.* (2019) **4**:14. https://doi.org/10.1007/s41024-019-0053-9.

[20]   Ferretti F., Incerti A., Ferracuti B., Mazzotti C. FRCM strengthened masonry panels: the role of mechanical anchorages and symmetric layouts. *Key Eng. Mater.* (2017) **747**:334–341.

[21]   Del Zoppo M., Di Ludovico M., Prota A. Analysis of FRCM and CRM parameters for the in-plane shear strengthening of different URM types. *Compos. B Eng.* (2019) **171**:20–33.

[22]   ASTM E519−15. Standard test method for diagonal tension (shear) in masonry assemblages 2015:4–8. https://doi.org/10.1520/E0519.

[23]   RILEM LUMB6. Diagonal tensile strength tests of small wall specimens. *RILEM TC-76 LUM* (1991).

[24]   EN 772-1. Methods of test for masonry units - Part 1: Determination of compressive strength (2011).

[25]   EN 12390-6:2009. Testing hardened concrete - Part 6: Tensile splitting strength of test specimen (2009).

[26]   EN 12390-5:2009. Testing hardened concrete - Part 5: Flexural strength of test specimens (2009).

[27]   EN 12390-13. Testing hardened concrete - Determination of secant modulus of elasticity in compression (2013).

[28]   EN 1015-11:1999/A1:2006. Methods of test for mortar for masonry - Part 11: Determination of flexural and compressive strength of hardened mortar (2006).

[29]   Frocht, M. Recent advances in photoelasticity. *ASME Trans* (1931) **55**:135–53.

[30]   Yokel, F.Y. and Fattal, S.G. A Failure hypothesis for masonry shearwalls. J. Struct. Div. - ASCE (1976) **102**:515–32.

[31]   CNR-DT 215/2018. Istruzioni per la Progettazione, l'Esecuzione ed il Controllo di Interventi di Consolidamento Statico mediante l'utilizzo di Compositi Fibrorinforzati a Matrice Inorganica (in Italian). *National Research Council (CNR)* (2018).